Simulation of Action Potentials From Metabolically Impaired Cardiac Myocytes

Role of ATP-Sensitive K^+ Current

José M. Ferrero, Jr, Javier Sáiz, José M. Ferrero, Nitish V. Thakor

Abstract The role of the ATP-sensitive K^+ current ($I_{K\text{-}ATP}$) and its contribution to electrophysiological changes that occur during metabolic impairment in cardiac ventricular myocytes is still being discussed. The aim of this work was to quantitatively study this issue by using computer modeling. A model of $I_{K\text{-}ATP}$ is formulated and incorporated into the Luo-Rudy ionic model of the ventricular action potential. Action potentials under different degrees of activation of $I_{K\text{-}ATP}$ are simulated. Our results show that in normal ionic concentrations, only ≈0.6% of the K_{ATP} channels, when open, should account for a 50% reduction in action potential duration. However, increased levels of intracellular Mg^{2+} counteract this shortening. Under conditions of high $[K^+]_o$, such as those found in early ischemia, the activation of only ≈0.4% of the K_{ATP} channels could account for a 50% reduction in action potential duration. Thus, our results suggest that opening of $I_{K\text{-}ATP}$ channels should play a significant role in action potential shortening during hypoxic/ischemic episodes, with the fraction of open channels involved being very low (<1%). However, the results of the model suggest that activation of $I_{K\text{-}ATP}$ alone does not quantitatively account for the observed K^+ efflux in metabolically impaired cardiac myocytes. Mechanisms other than K_{ATP} channel activation should be responsible for a significant part of the K^+ efflux measured in hypoxic/ischemic situations. (***Circ Res.*** **1996;79:208-221.**)

Key Words • computer model • ATP-regulated channels • myocardial ischemia • action potential shortening • K^+ efflux

It is well known that myocardial hypoxia and ischemia cause profound changes in the electrophysiological properties of cardiac tissue. One of the major changes that occur in ventricular muscle cells during metabolic impairment is shortening of the AP.[1] The reduction of APD initially causes a shortening of the refractory period,[2] and this can facilitate the appearance of reentrant-type arrhythmias.[2] The reduction of APD during ischemia can partly be explained by an increased $[K^+]_o$,[3,4] but additional factors seem to be involved in AP shortening. Indeed, during hypoxic perfusion, the AP is known to shorten in the absence of extracellular K^+ accumulation.[1,5]

Since K_{ATP} channels were first described by Noma,[6] their contribution to the shortening of the AP during hypoxia and ischemia and to other electrophysiological changes has been debated and is still not completely clarified. The major argument against the role of the K_{ATP} channels during early ischemia is that the value of $[ATP]_i$ needed to open 50% of the channels is two orders of magnitude below the measured $[ATP]_i$ bulk level in the first phase of ischemia.[7] Thus, the fraction of channels activated during early ischemia is likely to be very low, and from this point of view, the current carried by K_{ATP} channels ($I_{K\text{-}ATP}$) might not seem to contribute significantly to the AP shortening and other ischemia-related electrophysiological changes.[4,7] Moreover, because $I_{K\text{-}ATP}$ channel blockers, such as glibenclamide, only partially prevent hypoxic/ischemic AP shortening, it has been suggested that currents other than $I_{K\text{-}ATP}$ must significantly contribute to APD reduction.[8,9]

On the other hand, it has also been suggested that only a small number of K_{ATP} channels need to be activated to account for the changes observed in AP configuration. Following this "spare-channel hypothesis" suggested by Cook et al,[10] several investigators have found indirect experimental evidence that supports this idea in the case of cardiac myocytes.[11-14] However, because of the difficulty of experimentally measuring the fraction of open K_{ATP} channels directly, there is still no direct proof of this hypothesis, and the quantitative importance of $I_{K\text{-}ATP}$ channel opening in hypoxic/ischemic episodes is not yet completely established.

The contribution of $I_{K\text{-}ATP}$ to cellular K^+ loss during hypoxic/ischemic situations is not clear either. There exists experimental evidence that supports the idea that $I_{K\text{-}ATP}$ channel activation largely[14,15] or partially[16,17] accounts for K^+ loss from the cell in the first minutes of a hypoxic/ischemic episode. However, the ineffectiveness of K^+ channel openers to enhance the rate of K^+ loss[18,19] and the dissociation between K^+ efflux, AP shortening, and intracellular ATP levels in hypoxia/ischemia,[4] among others,[20] are reasons against a major role of $I_{K\text{-}ATP}$ in this phenomenon.

The main goal of the present study was to use a computer model to quantitatively study the influence of $I_{K\text{-}ATP}$ on changes in AP configuration and cellular K^+ loss in metabolically impaired conditions. For this purpose, we have formulated a detailed model of this current and have incorporated it into the LR-II model[21] of the guinea pig–

Received November 27, 1995; accepted May 10, 1996.

From the Laboratorio Integrado de Bioingeniería (J.M.F. Jr, J.S., J.M.F.), Departamento de Ingeniería Electrónica, Universidad Politécnica de Valencia, Valencia, Spain, and the Department of Biomedical Engineering (J.M.F. Jr, J.S., N.V.T.), The Johns Hopkins University, Baltimore, Md.

Reprint requests to Dr José María Ferrero, Jr, Laboratorio Integrado de Bioingeniería, Universidad Politécnica de Valencia, Camino de Vera s/n, 46020 Valencia, Spain. E-mail cferrero@pleiades.upv.es.

Selected Abbreviations and Acronyms

AP = action potential
APD = AP duration
BCL = basic cycle length
f_{ATP} = fraction of open K_{ATP} channels
$I_{K,O}$ = total outward K^+ current
$I_{K,T}$ = total K^+ current
$I_{K\text{-}ATP}$ = ATP-sensitive K^+ current
$I_{K\text{-}R}$ = sum of K^+ currents not including $I_{K\text{-}ATP}$
I_{K1} = inward rectifier K^+ current
J_{efflux} = K^+ unidirectional efflux rate
ΔJ_{efflux} = net increment in K^+ unidirectional efflux rate
K_{ATP} channel = ATP-sensitive K^+ channel
LR-II model = phase II Luo-Rudy model
V_{ECW} = extracellular water volume
V_m = membrane potential

type ventricular cardiac AP. We use this model to study the relationship between APD and intracellular nucleotide levels and ionic concentrations. The influence of $I_{K\text{-}ATP}$ activation on reduction of APD during ischemia in the presence of high $[K^+]_o$ has been theoretically elucidated. Finally, the contribution of $I_{K\text{-}ATP}$ to the increase in the rate of K^+ efflux in hypoxia/ischemia is also theoretically investigated.

Materials and Methods

Model of $I_{K\text{-}ATP}$

General Considerations

The mathematical model of $I_{K\text{-}ATP}$ that we formulate here is based on different sets of published experimental data describing the dependence of the channel current density on ion concentrations ($[K^+]_o$, $[Mg^{2+}]_i$, and $[Na^+]_i$) and intracellular nucleotide levels ($[ATP]_i$ and $[ADP]_i$). The parameters of the model are estimated, when necessary, using a linear least-squares method to fit the experimental data. The complete set of equations of the model is given in Appendix 1.

Current Density

The general equation describing the current density ($\mu A/cm^2$) is as follows:

$$(1) \qquad I_{K\text{-}ATP}=\sigma g_0 p_o f_{ATP}(V_m-E_{K\text{-}ATP})$$

where σ is the channel density, g_0 is the unitary conductance of a fully activated individual channel, p_o is the open probability of a channel in the absence of ATP, f_{ATP} is the fraction of activated channels (relative current), and V_m is the membrane potential. The term $E_{K\text{-}ATP}$ is the reversal potential of the channel, which is equal to the Nernst potential of K^+ ions[22] because of the specificity of the channel to K^+ ions in cardiac muscle cells.

We have used in our simulations a value of 3.8 channels/μm^2 for the channel density (derived from data in Reference 14), a value that is intermediate in the range of reported values for guinea pig ventricular myocytes. The open probability in the absence of ATP was assumed to be 0.91.[17] The sensitivity of the results to these parameters is discussed later.

Unitary Conductance

The expression for the unitary conductance (g_0) of an individual K_{ATP} channel is as follows:

$$(2) \qquad g_o([Mg^{2+}]_i, [Na^+]_i, [K^+]_o, V_m, T)=\gamma_0 f_M f_N f_T$$

where γ_0 is the unitary conductance in the absence of intracellular Na^+ and Mg^{2+}, f_M and f_N are nondimensional factors that account for the inward rectification of the channel, and f_T is a nondimensional temperature (T)-dependent factor.

The value of γ_0 is known to depend on $[K^+]_o$.[22,23] In the present model, we have used the formulation provided in Reference 22 (see Equation 10 of Appendix 1), which is widely accepted. On the other hand, K_{ATP} channels show inward rectification.[22,23] This property is the result of a voltage-dependent block caused by Na^+ and Mg^{2+} ions and obeys the laws of saturation kinetics.[23] We used this approach to express both factors f_M (for Mg^{2+}) and f_N (for Na^+) in Equation 2 by means of Hill-type equations (see Equations 11 and 14 in Appendix 1). The half-maximal saturation constants ($K_{h,ion}$) are given by Eyring rate theory:

$$(3) \qquad K_{h,ion}=K^0_{h,ion}\exp\left(-\frac{z_{ion}\delta_{ion}F}{RT}V_m\right)$$

where the subscript "ion" stands for Mg^{2+} and Na^+, respectively, $K^0_{h,ion}$ is the value of $K_{h,ion}$ at zero membrane voltage, δ_{ion} is the electrical distance, z_{ion} is the valence of the considered ion, F is the Faraday constant, R is the gas constant, and T is the absolute temperature. The values of the parameters used in our simulations and the details of the equations are listed in Appendix 1.

It is known that increasing levels of extracellular K^+ partially remove the voltage-dependent block caused by Mg^{2+} ions.[23] This fact was considered in our model by making $K^0_{h,Mg}$ increase monotonically with $[K^+]_o$ following a square-root dependence (see Equation 13 in Appendix 1) to fit data from Horie et al.[23]

Finally, a temperature-dependent term, f_T, was introduced by using a temperature coefficient $Q_{10}=1.3$ (see Equation 16 in Appendix 1).[23]

Fig 1A illustrates the results obtained with the model of the unitary conductance in terms of the current-voltage relationships of the channel. The symbols in both plots represent experimental values corresponding to different values of $[K^+]_o$ (data duplicated from Reference 24). The solid lines represent the curves predicted by the model.

Nucleotide Dependence

It is well known that when intracellular ATP molecules bind to the channel protein, it becomes inactivated. Thus, f_{ATP} in a myocyte strongly depends on $[ATP]_i$. Experimental data[6,12,14,25,26] are properly fitted by means of a Hill-type equation:

$$(4) \qquad f_{ATP}=\frac{1}{1+([ATP]_i/K_m)^H}$$

where K_m is the half-maximum inhibition constant and H is the Hill coefficient.

Several factors related to the metabolic state of the cell modulate the $[ATP]_i$ dependence of f_{ATP} (for a review, see Reference 27). Among them, free cytosolic ADP is known to stimulate partially inactivated channels in the presence of Mg^{2+}.[14,25,28] Both the half-maximal inhibition constant (K_m) and the Hill coefficient of Equation 4 are dependent on free $[ADP]_i$. Using the data reported by Weiss et al,[14] we have modeled the dependence of f_{ATP} on $[ADP]_i$. Specifically, we used the average values of K_m and Hill coefficients for individual membrane patches obtained by Weiss et al for different values of $[ADP]_i$. The mathematical expressions that result from the best fit are given in Appendix 1 (see Equations 18 and 19); they show a monotonic increase of K_m and a monotonic decrease of the Hill coefficient with $[ADP]_i$, respectively.

The fraction of open channels will depend, in this way, on intracellular concentrations of both ATP and ADP. Fig 1B graphically illustrates this dependence in an appropriate way to easily relate nucleotide levels to f_{ATP} values. Indeed, these curves can be used to "translate" a given value of f_{ATP} to the different combinations of $[ATP]_i$-$[ADP]_i$, which, when present in the cell, give rise to such a value of f_{ATP}. Each curve in the figure can be regarded, then, as an "isoactivation" curve for $I_{K\text{-}ATP}$.

Model of the Ventricular AP

Once the model for $I_{K\text{-}ATP}$ was formulated, we incorporated it into the LR-II model described by Luo and Rudy.[21] This mathematical model reproduces the AP of endocardial ventricular myocytes of guinea pig–type hearts with a high degree of electrophysiological detail. It includes mathematical descriptions of 12 different ionic currents, as well as intracellular Ca^{2+} buffering and the Ca^{2+}-induced Ca^{2+} release process. The basic equation that relates V_m to ionic currents is the following:

$$C_m \frac{dV_m}{dt} + \Sigma I_{ion} + I_{stim} = 0 \quad (5)$$

where C_m is the membrane capacitance, I_{stim} is the stimulus current, and ΣI_{ion} is the sum of all the ionic currents that cross the sarcolemma, namely, the fast Na^+ current (I_{Na}), the current through the L-type Ca^{2+} channels ($I_{Ca,L}$),* the delayed rectifier K^+ current (I_K), the inward rectifier K^+ current (I_{K1}), the plateau K^+ current (I_{Kp}), the Na^+-Ca^{2+} exchanger current (I_{NaCa}), the Na^+-K^+ pump current (I_{NaK}), a nonspecific Ca^{2+}-activated K^+ and Na^+ current (I_{ns}), and the current carried by the sarcolemmal Ca^{2+} pump ($I_{p(Ca)}$). Mathematical details of this model can be found elsewhere.[21]

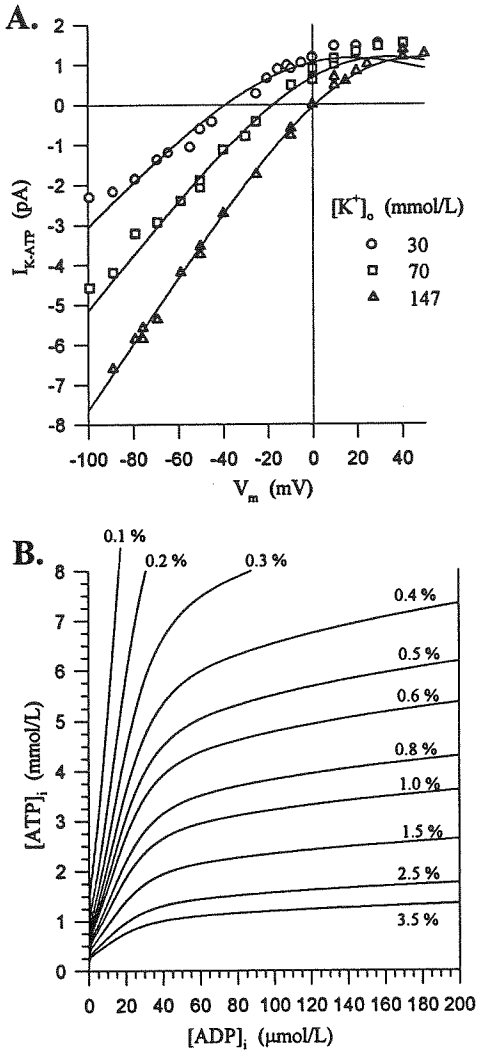

FIG 1. Characteristics of K_{ATP} channels considered in the model. A, Single-channel current-voltage relationships for the K_{ATP} channel. In this figure, $I_{K\text{-}ATP}$ is the current through a single fully activated channel. Symbols indicate experimental values (duplicated from Fig 6A in Reference 24); solid lines are simulation results. Each plot corresponds to a different value of $[K^+]_o$. Intracellular concentrations of Na^+, K^+, and Mg^{2+} are 8, 140, and 3.1 mmol/L, respectively. B, f_{ATP} as a function of $[ATP]_i$ and $[ADP]_i$. Equations 4, 12, and 13 were used to generate these plots. Each curve corresponds here to a certain value of f_{ATP} (indicated in percentage above each curve).

Normal Ionic Concentrations

Ion	Concentration, mmol/L		
	Intracellular	Extracellular	Bulk
Na^+	10	140	140
Ca^{2+}	0.12×10^{-3}	1.8	1.8
K^+	145	5.4	5.4
Mg^{2+}	0.5	...	...

In our simulations, extracellular ionic concentrations were held constant, unless otherwise noted (see "Extracellular K^+ Accumulation" below). Intracellular concentrations changed dynamically as a result of ionic fluxes through the sarcolemma. The normal values of extracellular concentrations and initial intracellular concentrations are listed in the Table. All simulations correspond to a temperature of 37°C.

Stimulation Protocol

In each simulation, unless otherwise noted (see "Extracellular K^+ Accumulation" below), constant values were assigned to each relevant parameter of the model (ie, f_{ATP} and ionic concentrations), and in these conditions, the cell was stimulated with a constant BCL. In order to achieve steady state conditions and to avoid alternants in APD, 10 APs were elicited before recording the data. The stimulus consisted of rectangular current pulses 2 ms in duration and an amplitude 1.5 times the diastolic threshold.

APD

We defined APD in our simulations as the interval between the instant of maximum upstroke velocity of the AP, $[dV/dt]_{max}$, and the instant of 90% repolarization.

Calculation of J_{efflux}

When calculating the rate of K^+ efflux from the cell, the basic LR-II model was slightly modified so as to achieve zero net K^+ efflux under basal normoxic conditions. Specifically, the maximum current density through the Na^+-K^+ pump was increased from 1.5 to 2.61 $\mu A/\mu F$, which is still in the range of measured values.[29] This change affects AP morphology only slightly (small decrease of APD due to accelerated repolarization).

To compute J_{efflux}, we started by subtracting the K^+ (inward) current carried by the Na^+-K^+ pump from the total K^+ current ($I_{K,T}$) to obtain the total outward K^+ current ($I_{K,O}$). Taking into account the 3:2 stoichiometry of the pump, this results in $I_{K,O}=I_{K,T}+2I_{NaK}$ (where I_{NaK} is the Na^+-K^+ pump current). We then calculated the average outward current density (I_{out}) as the integral mean value of $I_{K,O}$. In order to compare the simulation results with experimental data, the current density value was translated to J_{efflux} (in $\mu mol\cdot g^{-1}\cdot min^{-1}$) using the following expression:

$$J_{efflux} = \frac{600\,000}{F}\left(\frac{1}{\rho} - V_{ECW}\right) S_v I_{out} \quad (6)$$

The assumed values of the parameters in Equation 6 were $\rho=1$ kg/L for the myocardial density, $V_{ECW}=0.52$ L/kg wet wt for the

*Note that the correct formulation of the term f_∞, which appears in the L-type Ca^{2+} current formulation, is given in the text of the article by Luo and Rudy[21] (page 1073) and not in the list of equations at the end of said article.

extracellular water content,[30] and S_v=0.3 $\mu m^2/\mu m^3$ for the surface-to-volume ratio of the myocyte. F stands for the Faraday constant. Details about derivation of Equation 6 can be found in Appendix 2.

Finally, ΔJ_{efflux} was calculated as the difference between the actual value of J_{efflux} and its control value (corresponding to f_{ATP}=0%).

Extracellular K^+ Accumulation

We also carried out long simulations in which extracellular K^+ accumulation was studied. In these simulations, the cell was paced with a BCL of 800 ms, and f_{ATP} was either abruptly or gradually increased. Extracellular concentrations were permitted to change dynamically as a result of ionic fluxes through the cellular membrane. A three-compartment model was assumed, and diffusion of ions from the extracellular cleft to the bulk extracellular medium was considered. Thus, ionic concentrations in the cleft can be described by the following equation:

$$(7)\quad \frac{d[S]_o}{dt}=\frac{S_v}{V_{ECW}z_S F}\left(\frac{1}{\rho}-V_{ECW}\right)I_{S,total}-\frac{[S]_{bulk}-[S]_o}{\tau_{diff}}$$

where $[S]_o$ and $[S]_{bulk}$ are the concentrations of the ionic species S in the extracellular cleft and in the bulk extracellular medium, respectively. The term z_S is the valence of the ionic species S, and $I_{S,total}$ stands for the total current through the sarcolemma carried by the ionic species S. Finally, τ_{diff} (1 s) is the time constant associated with the diffusion of ions from the cleft to the bulk extracellular medium.

When simulating extracellular K^+ accumulation during no-flow ischemia, the diffusion term in Equation 7 was omitted (τ_{diff}) to account for the lack of flow.

The modified version of the Na^+-K^+ pump in the LR-II model was also used in the simulations (see "Calculation of J_{efflux}" above).

Computation Methods

Programs were written in ACSL language using Gear stiff algorithm[31] to solve the nonlinear system of differential equations that results from the AP model. Simulations were carried out in a SUN SparcStation 1 using double-precision variables. To ensure numerical accuracy, the maximum allowed time step was 10 μs. The maximum relative error allowed for every variable in each iteration was 10^{-6}.

Results

In all the simulations that are presented in this section, f_{ATP} is varied, and the effect of this variation on AP configuration, ionic currents, and K^+ efflux is investigated. A given value of f_{ATP} can be related to $[ATP]_i$ and $[ADP]_i$ using the isoactivation curves shown in Fig 1B.

Effects of K_{ATP} Channel Opening on AP Configuration and Ionic Currents

The effects of the progressive activation of $I_{K\text{-}ATP}$ on the characteristics of the ventricular AP were first investigated using normal nonischemic values for the ionic concentrations. The values used are listed in the Table.

Fig 2 shows the results of these simulations. In Fig 2A, a set of APs that correspond to different values of f_{ATP} is shown. It can be noted that AP configuration varies significantly when K_{ATP} channels become activated, even with very low values of f_{ATP}. When f_{ATP} increases, there is a marked reduction in APD, a moderate reduction of the plateau potential, and a slight diastolic hyperpolarization. Resting V_m, whose value is −86.5 mV in control (f_{ATP}=0%) conditions, decreases almost linearly to reach a value of −87.1 mV for f_{ATP}=2.5%. This would be in

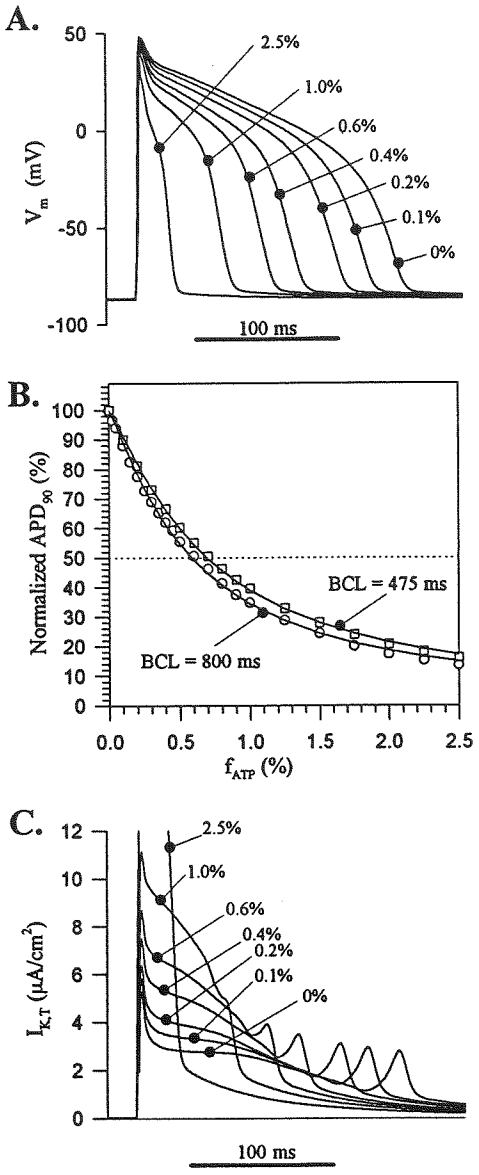

FIG 2. Results of the model under conditions of normal ionic concentrations (see Table). A, Simulated APs for different values of f_{ATP} (numbers indicated, in percentage, for each curve). The cell was electrically stimulated with a BCL of 800 ms. B, Normalized APD as a function of f_{ATP} for two different BCLs (475 and 800 ms). APD is normalized in each case to its control value (184.1 ms for BCL=800 ms, and 175.2 ms for BCL=475 ms), which corresponds to f_{ATP}=0%. C, Time course of the total K^+ current crossing the sarcolemma ($I_{K,T}$, calculated as the net sum of all K^+ currents carried by sarcolemmal K^+ channels and pumps) for different degrees of K_{ATP} channel activation. The same BCL as in panel A was used.

accordance with the slight diastolic hyperpolarization observed by Gasser and Vaughan-Jones[15] in myocytes exposed to hypoxic conditions, although other studies have reported opposite results.[32] The cell becomes completely unexcitable for $f_{ATP}\approx$3.1% for the standard stimulus used in the simulations (not shown).

The reduction in APD caused by increasing activation of $I_{K\text{-}ATP}$ is represented in Fig 2B, in which the results corresponding to two different BCLs are compared. For each BCL, the APD has been normalized to its maximum value, which corresponds to the complete inactivation of

the K_{ATP} channels. For a BCL of 800 ms, the figure shows how the activation of ≈0.6% of the total population of channels is sufficient to account for a 50% shortening in APD. This figure increases to ≈0.7% when the pacing frequency is increased to a BCL of 475 ms.

The value of f_{ATP} needed to shorten APD to half its control value is in accordance with several experimental results.[11,13,14] Moreover, the rate of change of APD with f_{ATP} agrees very nicely with indirect experimental findings by Nichols and Lederer.[12]

Activation of $I_{K\text{-}ATP}$ modifies the ionic sarcolemmal currents significantly. Fig 2C shows the evolution of the total K^+ current ($I_{K,T}$) as activation of $I_{K\text{-}ATP}$ progresses. The total time during which the K^+ currents are flowing shortens in correspondence with the reduction in APD. Both the maximum peak of $I_{K,T}$ and the amplitude of the K^+ current "plateau" increase with f_{ATP}. The secondary peak of the K^+ current in phase 3, mainly due to activation of the time-independent I_{K1}, also increases, although only slightly, with f_{ATP}.

Fig 3 depicts the relative contributions of $I_{K\text{-}ATP}$ and the rest of the sarcolemmal K^+ currents to $I_{K,T}$. The time courses of $I_{K\text{-}ATP}$ and of the sum of all the other K^+ currents ($I_{K\text{-}R}$) are compared for six different values of f_{ATP}. The shape of $I_{K\text{-}ATP}$ is a distorted version of the AP waveform, due to the inward rectification of the K_{ATP} channels, and presents a plateau whose level is proportional to the degree of channel activation. Regarding $I_{K\text{-}R}$, both the initial peak during depolarization (due mainly to the plateau K^+ current and to I_{K1}) and the secondary peak during repolarization (due basically to I_{K1}) are practically independent of f_{ATP}. Opening of K_{ATP} channels significantly depresses the plateau of $I_{K\text{-}R}$. It is noticeable that for degrees of K_{ATP} channel activation over 0.4%, the overall contribution of $I_{K\text{-}ATP}$ to $I_{K,T}$ is higher than the contribution of all the rest of the K^+ currents added together.

Effects of Changes on Ionic Concentrations

In the next set of simulations, $[Mg^{2+}]_i$, $[Na^+]_i$, and $[K^+]_o$ are varied in turn while the other ionic concentrations remain at their control levels (see the Table). The effects of changes in these concentrations, which modulate the activity of the K_{ATP} channels, on AP configuration and APD are further investigated.

Changes in $[Mg^{2+}]_i$

Myoplasmic free Mg^{2+}, which partially blocks K_{ATP} channels in a voltage-dependent fashion, is known to increase from its control level (≈0.5 mmol/L) to ≈2.5 mmol/L in 6 to 9 minutes of global ischemia.[33] To investigate the effects of increased intracellular Mg^{2+} level on AP configuration, we simulated APs under different K_{ATP} channel activation degrees for three different $[Mg^{2+}]_i$ levels. The results are shown in Fig 4. Each of the six sets of APs plotted in Fig 4A corresponds to a fixed value of f_{ATP}. It can be seen that increased levels of intracellular Mg^{2+} partially counteract the AP shortening caused by $I_{K\text{-}ATP}$. High $[Mg^{2+}]_i$ also elevates the AP plateau level because of the enhanced inward rectification of the K_{ATP} channels.

The relationship between normalized APD and f_{ATP} for different $[Mg^{2+}]_i$ levels is plotted in Fig 4B. Note that the effect of intracellular Mg^{2+} on APD is more significant at higher values of f_{ATP}. The fraction of channels needed to be activated to reduce APD to 50% rises from ≈0.6% for $[Mg^{2+}]_i$=0.5 mmol/L to ≈0.8% for $[Mg^{2+}]_i$=1.5 mmol/L and ≈1.0% for $[Mg^{2+}]_i$=2.5 mmol/L. The current through K_{ATP} channels at V_m=0 mV is reduced from 80% to 46% of the maximum possible current when $[Mg^{2+}]_i$ increases from 0.5 to 2.5 mmol/L. According to these results, the effect of an increased intracellular Mg^{2+} level during hypoxia/ischemia has a considerable effect on APD, reducing the K_{ATP}-mediated shortening of the AP.

Changes in $[Na^+]_i$

Next, we investigated the effects of increased levels of intracellular Na^+. APs corresponding to different values of $[Na^+]_i$ and different values of f_{ATP} are shown in Fig 5A. Changes in $[Na^+]_i$ have two different effects on AP configuration. The first one is independent of K_{ATP} channels and is due to the dependence on $[Na^+]_i$ exhibited by several ionic channels, pumps, and exchangers in the sarcolemma.[21] This direct effect tends to shorten the AP when intracellular levels of Na^+ rise, even in the absence of K_{ATP} channel activation. Fig 5B, which shows the dependence of APD on f_{ATP} for three different values of $[Na^+]_i$, illustrates this phenomenon. All APDs are referred to the value that corresponds to f_{ATP}=0% and $[Na^+]_i$=10 mmol/L. Note, indeed, that for any constant value of f_{ATP}, AP shortens as $[Na^+]_i$ increases. On the other hand, as discussed previously, intracellular Na^+ causes a partial voltage-dependent block in K_{ATP} channels. This would tend to reduce the AP shortening caused by $I_{K\text{-}ATP}$ activation, as happens with intracellular Mg^{2+}. To further investigate this effect,

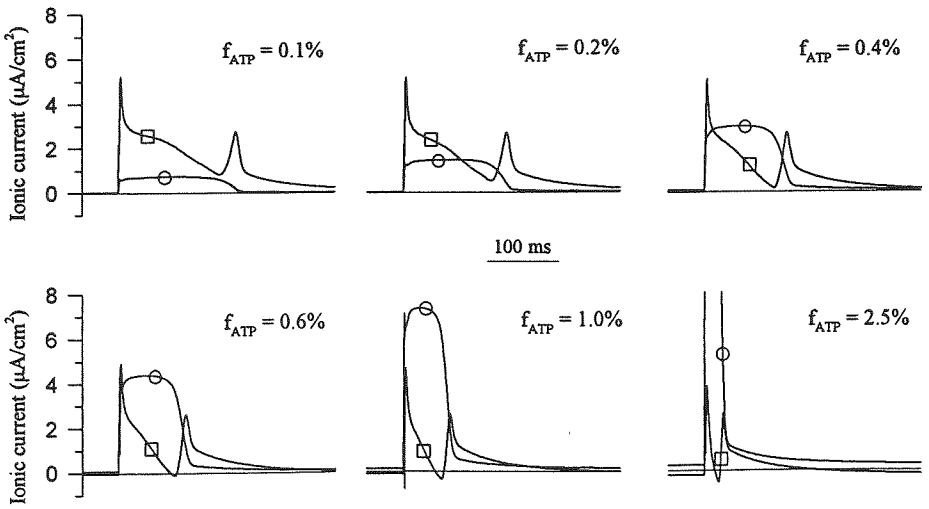

FIG 3. Time course of K^+ currents for different values of f_{ATP}. Ionic concentrations are listed in the Table. ○ indicates $I_{K\text{-}ATP}$; □, $I_{K\text{-}R}$.

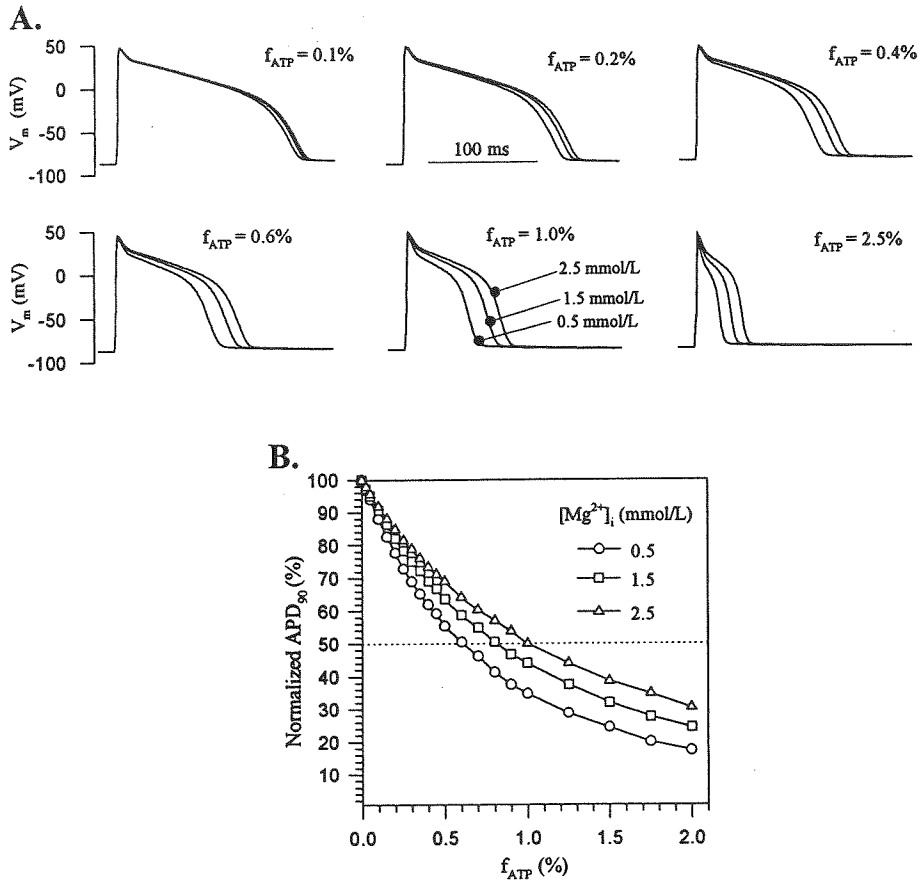

FIG 4. Effect of intracellular Mg^{2+} levels on AP configuration. A BCL of 800 ms was used in the simulations. Ionic concentrations other than $[Mg^{2+}]_i$ are listed in the Table. A, Simulated APs corresponding to different degrees of K_{ATP} channel activation (values of f_{ATP} are indicated above each set). The longest of the three APs on each panel corresponds to $[Mg^{2+}]_i$=2.5 mmol/L; the central one, to 1.5 mmol/L; and the shortest one, to 0.5 mmol/L. B, Normalized APD as a function of f_{ATP} for three different values of $[Mg^{2+}]_i$. Control value of APD (100% level) is 184.1 ms.

we constructed Fig 5C by normalizing APD values in a different way. Each value of APD corresponding to a given level of intracellular Na^+ was normalized to the maximum APD value (corresponding to f_{ATP}=0%) found under that particular $[Na^+]_i$. In this way, the direct effect of intracellular Na^+ previously mentioned is eliminated, while the K_{ATP}-dependent effect is maintained and amplified. When APD values are normalized in this manner, it can be seen (Fig 5C) that all the curves (APD versus f_{ATP}) fall reasonably well on a single curve, with maximum differences in APD values being in the range of 5% for all values of f_{ATP}. This means that the effect of $[Na^+]_i$ on APD mediated by K_{ATP} channels is very small in the range of $[Na^+]_i$ tested. Note that the current through K_{ATP} channels at V_m=0 mV is reduced from 87% to 63% of the maximum possible current when $[Na^+]_i$ is increased from 10 to 20 mmol/L, which is much less significant than the reduction caused by Mg^{2+}.

Changes in $[K^+]_o$

Increases in $[K^+]_o$ that take place in ischemic episodes are known to profoundly affect APD. The effects of high $[K^+]_o$ on APD are mediated in part by an increase in the conductance of both the inward rectifier (g_{K1}) and the delayed rectifier (g_K) channels, something which tends to decrease APD. Similarly, $[K^+]_o$ is also known to affect the conductance of K_{ATP} channels in a similar manner.[22]

We used the model to investigate the effect of $[K^+]_o$ on AP configuration for different degrees of activation of $I_{K\text{-}ATP}$. Fig 6 depicts the results obtained. The upper left APs in Fig 6A correspond to complete inactivation of $I_{K\text{-}ATP}$, and it is seen, as expected, how APD reduces in response to increases in $[K^+]_o$. APs also exhibit diastolic depolarization, which is due to the increase in $[K^+]_o$. The other five sets of APs in Fig 6A show the effects of the progressive activation of $I_{K\text{-}ATP}$ on AP configuration. As f_{ATP} increases, APD is further decreased, resting V_m is scarcely affected, and the absolute influence of $[K^+]_o$ on APD is reduced.

Fig 6B shows the effect of $[K^+]_o$ on the APD-f_{ATP} dependence. APD values are normalized to the reference value corresponding to f_{ATP}=0% and $[K^+]_o$=5.4 mmol/L. The fraction of open K_{ATP} channels needed to produce a 50% reduction in APD is reduced from ≈0.6% to 0.55%, 0.48%, and 0.38% as $[K^+]_o$ increases from 5.4 mmol/L to 7.5, 9.5, and 11.5 mmol/L, respectively.

However, if we normalize the values of APD for each value of $[K^+]_o$ to their control value (f_{ATP}=0%) corresponding to that particular $[K^+]_o$, the results are different. As illustrated in Fig 6C, the relative reduction of APD normalized in this way is independent of $[K^+]_o$ (all the points fall reasonably well in one single curve). These results suggest that both high $[K^+]_o$ and K_{ATP} channel activation tend to reduce APD, but the effects of these two factors seem to be independent of one another. Indeed, Fig 6C shows that for any value of $[K^+]_o$ in the range of early ischemia, ≈0.6% of the total population of channels, when open, always cause a 50% reduction in APD from its control value independently of $[K^+]_o$. Similarly (although not shown in the figures), for a fixed value of f_{ATP} in the range of 0% to 2.5%, APD is reduced to 76% of its control value when $[K^+]_o$ increases from

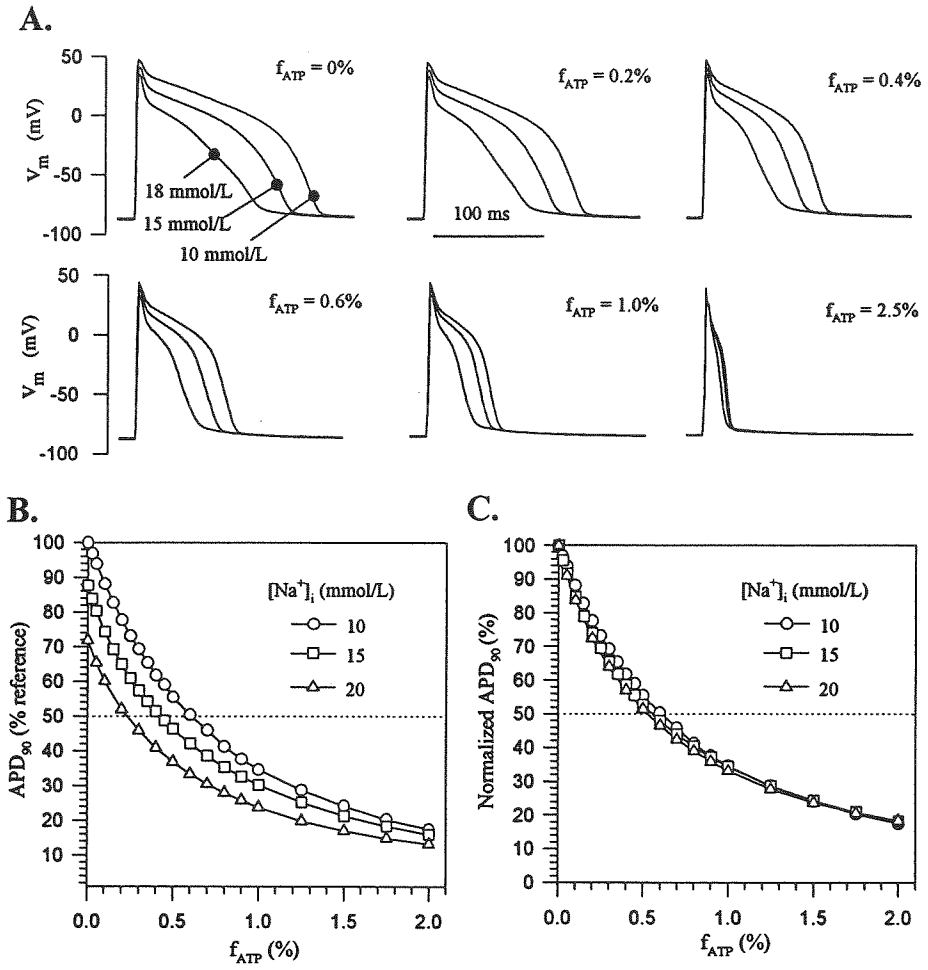

FIG 5. Effects of intracellular Na^+ on APD. A, Simulated APs corresponding to different degrees of K_{ATP} channel activation (values of f_{ATP} are indicated above each set). The longest of the three APs on each panel corresponds to $[Na^+]_i$=10 mmol/L; the central one, to 15 mmol/L; and the shortest one, to 18 mmol/L. B, Normalized APD as a function of f_{ATP} for three different values of $[Na^+]_i$. Control values of APD for each $[Na^+]_i$, corresponding to f_{ATP}=0%, are 184.1 ms ($[Na^+]_i$=10 mmol/L, 100% reference value), 161.4 ms ($[Na^+]_i$=15 mmol/L), and 132.2 ms ($[Na^+]_i$=20 mmol/L). The cell was stimulated with a BCL of 800 ms. Ionic concentrations other than $[Na^+]_i$ are listed in the Table. C, Same data as in panel B but normalized with a different criterion. For each value of $[Na^+]_i$, the normalized APD was referred to the corresponding control value specified above.

5.4 to 11.5 mmol/L, independently of the value of f_{ATP} considered.

Fig 6B can also be used to compare the separate effects of high $[K^+]_o$ and K_{ATP} channel activation on AP shortening. It is seen that in the range of values chosen for $[K^+]_o$ and f_{ATP}, the effect of K_{ATP} channel activation on AP shortening under conditions of normal $[K^+]_o$ is more pronounced than that of extracellular K^+ accumulation alone. In the absence of K_{ATP} channel activation, typical early ischemic levels of $[K^+]_o$ of 11 to 12 mmol/L[16] shorten the APD to ≈75% of its control value. On the other hand, activation of 0.6% of the total population of K_{ATP} channels, which might be a typical value in early ischemia (see "Discussion" and Reference 14), reduces APD to ≈50% in the presence of normal K^+ levels.

Cellular K^+ Loss

It is a well-known phenomenon that cardiac myocytes lose K^+ during metabolically impaired situations. In ischemic episodes, K^+ loss begins at ≈15 s after the onset of ischemia, and net K^+ efflux rate reaches a peak value in the range of 0.3 to 0.5 μmol/(g·min).[4,16] In substrate-free hypoxia, net K^+ loss averages 0.54 to 0.60 μmol/(g·min).[14,34] Finally, net K^+ efflux rate seems to be higher, ≈0.9 μmol/(g·min) in hypoxia with glucose present.[4]

The model presented here can be used to quantify the K^+ loss caused by the activation of $I_{K\text{-}ATP}$. For this purpose, we simulate APs for different pacing frequencies and different $[K^+]_o$ levels and quantify J_{efflux} and ΔJ_{efflux} using Equation 6 (see "Materials and Methods").

Fig 7A shows the magnitude of ΔJ_{efflux} (shown as ΔJ_T in Fig 7) as a function of f_{ATP} for two different values of BCL. As depicted in the figure, net increment in K^+ loss shows a biphasic behavior with K_{ATP} channel activation. Indeed, ΔJ_{efflux} initially increases with f_{ATP}, reaching a maximum value of 0.08 $\mu mol \cdot g^{-1} \cdot min^{-1}$ (BCL=800 ms) or 0.16 $\mu mol \cdot g^{-1} \cdot min^{-1}$ (BCL=475 ms) for f_{ATP} of ≈1%. From this point, ΔJ_{efflux} decreases as $I_{K\text{-}ATP}$ is further increased and even becomes negative for f_{ATP} >2.25% (BCL=800 ms) or 2.75% (BCL=475 ms).

The level of extracellular K^+ modulates the rate of K^+ loss from the cell, as demonstrated in Fig 7B, in which ΔJ_{efflux} is plotted against f_{ATP} for two different values of $[K^+]_o$. It is noticeable how the maximum ΔJ_{efflux} decreases when $[K^+]_o$ increases (0.081 $\mu mol \cdot g^{-1} \cdot min^{-1}$ for $[K^+]_o$=5.4 mmol/L, 0.044 $\mu mol \cdot g^{-1} \cdot min^{-1}$ for $[K^+]_o$=8.5 mmol/L). The degree of K_{ATP} channel opening for which the maximum takes place is also reduced (0.8% for $[K^+]_o$=5.4 mmol/L, 0.7% for $[K^+]_o$=8.5 mmol/L). Thus, in ischemic situations in which extracellular K^+ accumulation takes place, cellular K^+ loss through the K_{ATP} channels would be even smaller.

The rate of cellular K^+ loss mediated by $I_{K\text{-}ATP}$ obtained with the model is significantly lower than the values of total K^+ efflux found experimentally. Panels C and D of Fig 7 compare the simulation results with experimental measures of K^+ loss in different situations.[4,14,16,34] In Fig

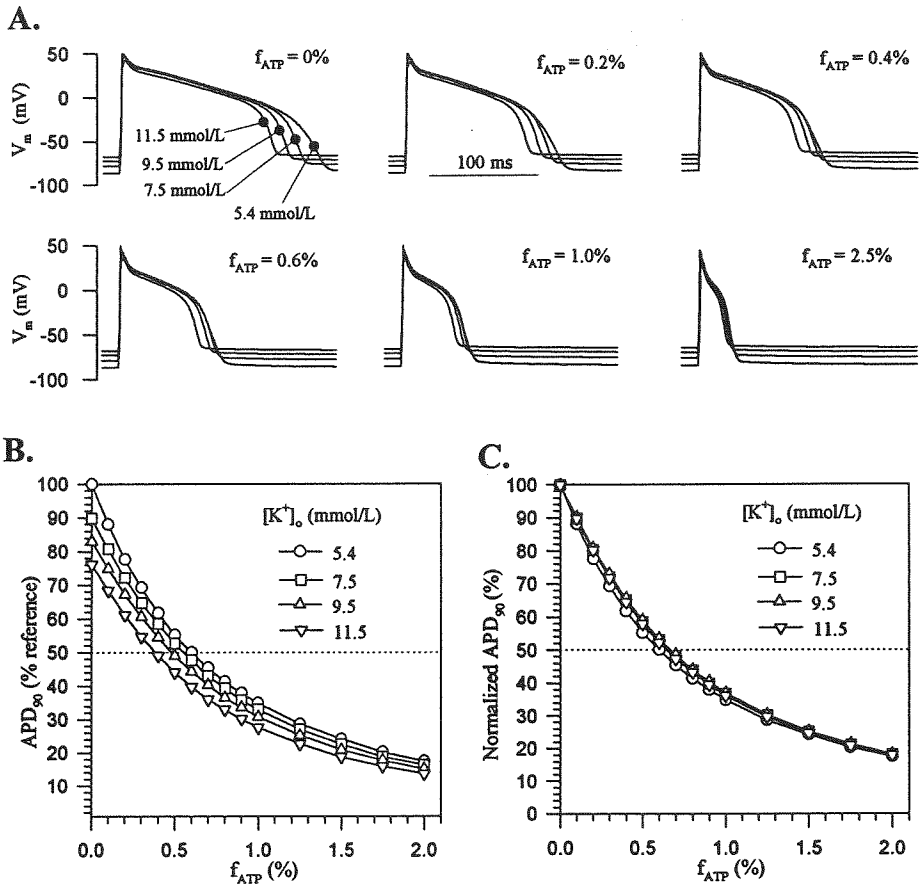

FIG 6. Effect of extracellular K^+ levels on AP configuration. Ionic concentrations other than $[K^+]_o$ are listed in the Table. A BCL of 800 ms was used in the simulations. A, Simulated APs corresponding to different degrees of K_{ATP} channel activation (values of f_{ATP} are indicated above each set). The longest of the four APs on each panel corresponds to $[K^+]_o$=5.4 mmol/L; the central ones, to 7.5 mmol/L and 9.5 mmol/L; and the shortest one, to 11.5 mmol/L. B, Normalized APD as a function of f_{ATP} for different values of $[K^+]_o$. Control values of APD for each $[K^+]_o$, corresponding to f_{ATP}=0%, are 184.1 ms ($[K^+]_o$=5.4 mmol/L, 100% reference value), 165.4 ms ($[K^+]_o$=7.5 mmol/L), 152.9 ms ($[K^+]_o$=9.5 mmol/L), and 140.3 ms ($[K^+]_o$=11.5 mmol/L). C, Same data as in panel B but normalized with a different criterion. For each value of $[K^+]_o$, the normalized APD was referred to the corresponding control value specified above.

7C, J_{efflux}, corresponding to a pacing frequency of 75 bpm (BCL=800 ms) obtained with the model, is compared with the experimental values obtained by Venkatesh et al[34] in similar experimental conditions. In normoxia, both theoretical and experimental values agree nicely (1.11 versus 1.24 $\mu mol \cdot g^{-1} \cdot min^{-1}$, respectively). However, in substrate-free hypoxia, the empirical J_{efflux} greatly exceeds the maximum theoretical K_{ATP}-related J_{efflux} (1.79 versus 1.18 $\mu mol \cdot g^{-1} \cdot min^{-1}$, respectively).

Fig 7D compares the values of ΔJ_{efflux} caused by $I_{K\text{-}ATP}$ activation, obtained with the model, with those obtained experimentally in different conditions. For the theoretical results, the maximum values of ΔJ_{efflux} in each situation have been chosen. The experimental values correspond to the peak of the K^+ efflux rate during the ischemic episode. It can be seen that, with only one exception, experimental values of ΔJ_{efflux} increase with pacing frequency. The figure shows that theoretical ΔJ_{efflux} through K_{ATP} channels is in the order of 5 to 7 times less than experimental values obtained in similar conditions. Thus, $I_{K\text{-}ATP}$ activation does not seem to quantitatively account for the entire observed hypoxic/ischemic cellular K^+ loss. All these results will be discussed in the next section.

Extracellular K^+ Accumulation

Many experimental studies have been published about the time course of $[K^+]_o$ during ischemia. There is general agreement in that, during early ischemia, $[K^+]_o$ initially increases and then plateaus at a level of ≈10 to 12 mmol/L.[4,14,20,30,35] This behavior can be qualitatively reproduced by the model, as seen in Fig 8. In Fig 8A, no-flow ischemia has been simulated by abruptly increasing f_{ATP} from 0% to 1.0%, while preventing K^+ diffusion from the extracellular cleft to bulk extracellular medium (see "Materials and Methods"). It can be noted from the figure that $[K^+]_o$ is approximately constant during normoxic perfusion (f_{ATP}=0%), because net K^+ efflux is zero in normal conditions. However, when K_{ATP} current becomes activated, $[K^+]_o$ rises until a steady state is reached (within minutes), when $[K^+]_o$ increases in a linear manner. This reflects the constant value of J_{efflux} in this situation (constant slope of ≈0.13 mmol/L per second, which corresponds to a J_{efflux} of 0.075 $\mu mol \cdot g^{-1} \cdot min^{-1}$).

In Fig 8B, no-flow ischemia is simulated in a more realistic manner. K_{ATP} channels are progressively (and linearly) activated from 0% to 2.5% during 10 minutes. In this time frame, $[K^+]_o$ increases from 5.4 to 8.0 mmol/L, reaching an approximately constant plateau.

Although the time course of $[K^+]_o$ shown in Fig 8B is qualitatively similar to those obtained experimentally, the values of $[K^+]_o$ reached are substantially smaller than the measured ones. Thus, again it is shown how, according to the model, ischemic K^+ loss through K_{ATP} channels does not account for the total observed cellular K^+ loss.

Discussion

The extent to which activation of $I_{K\text{-}ATP}$ contributes to the reduction of APD and to other electrophysiological changes during metabolically impaired situations still remains unanswered from a quantitative point of view. We have used a computer modeling approach to the problem to elucidate this issue. Although computer models cannot

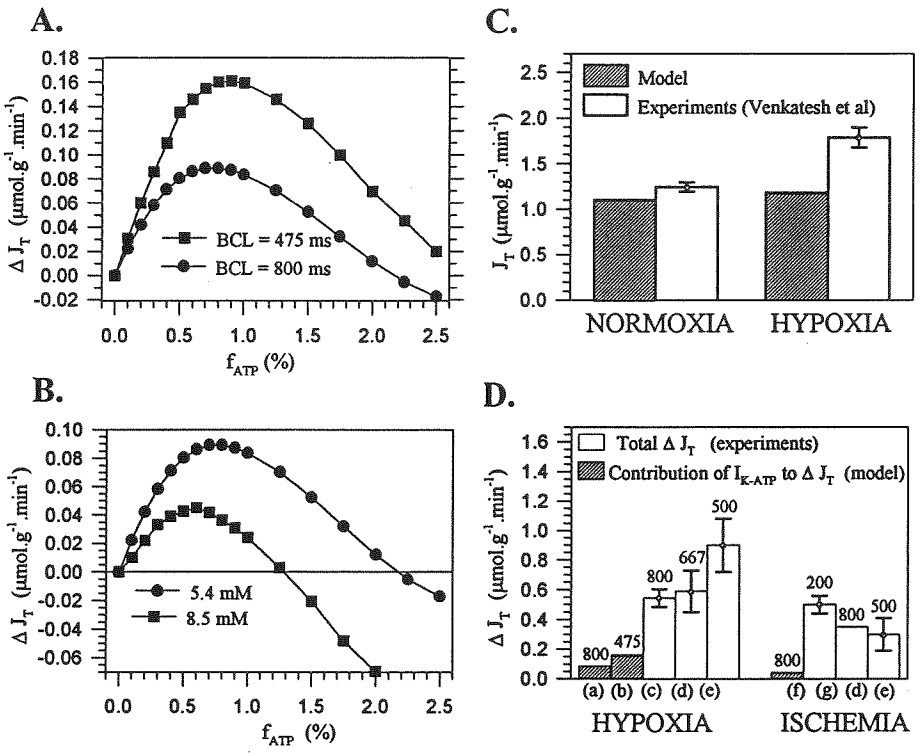

FIG 7. Model predictions regarding cellular K^+ loss related to K_{ATP} channel activation. A, Net increment in K^+ efflux rate (ΔJ_T) vs f_{ATP} for two values of BCL (indicated beside each curve) and normal ionic concentrations. B, Comparison between ΔJ_T values for two different extracellular K^+ levels (values of $[K^+]_o$ indicated beside each curve). BCL was 800 ms. C, Unidirectional K^+ efflux rates (J_T) in normally perfused conditions and in substrate-free hypoxia taken from Reference 34 compared with model results. In the simulations, "normoxia" corresponds to an f_{ATP} of 0%, and "hypoxia" corresponds to an f_{ATP} of 0.9%, which yields the maximum value of J_T. Ionic concentrations are those given in the Table. Both in simulations and in experiments, BCL was 800 ms. D, Values of ΔJ_T corresponding to different experimental results in hypoxic and ischemic situations compared with model results regarding the K_{ATP}-related K^+ loss. Numbers over each bar indicate the value (in milliseconds) of the BCL used in the simulation experiment. In simulation results, f_{ATP} yielding the maximum ΔJ_T was considered. In experimental ischemic results, the peak value of ΔJ_T in the ischemic period is represented. The abscissa is labeled as follows: a, simulation (f_{ATP}=0.9%, normal ionic concentrations); b, simulation (f_{ATP}=1.0%, normal ionic concentrations); c, data from Reference 34; d, data from Reference 14; e, data from Reference 4; f, simulation (f_{ATP}=0.7%, normal ionic concentrations except for $[K^+]_o$=8.5 mmol/L); and g, data from Reference 16.

provide real data, they can be used to make predictions and, in this case, can help us to understand the role of K_{ATP} channels in hypoxia-ischemia from a theoretical point of view.

The cardiac action potential model described by Luo and Rudy,[21] which has been used in the present study, is based on very recent patch-clamp data and reproduces membrane dynamics with a great degree of electrophysiological detail. The inclusion of a new formulation of the K_{ATP} current in this model makes it possible to simulate metabolically impaired situations more comprehensively.

Model of $I_{K\text{-}ATP}$

In its original form, the LR-II action potential model[21] does not include a mathematical description of $I_{K\text{-}ATP}$. The first goal of the present study was to formulate a comprehensive model for this current. Our description of $I_{K\text{-}ATP}$ is based on published experimental data regarding the main characteristics of the current.[14,17,22,23] We have integrated the available data regarding $I_{K\text{-}ATP}$ dependencies on $[K^+]_o$, $[Na^+]_i$, $[Mg^{2+}]_i$, $[ATP]_i$, and $[ADP]_i$ in a single set of equations. The model of $I_{K\text{-}ATP}$ finally formulated satisfactorily reproduces the main electrical features of K_{ATP} channels (eg, see Fig 1A and compare with Fig 6A of Reference 24). Other factors not considered in the model have been ignored because of their presumed lack of a physiological role during the early phase of hypoxia/ischemia (eg, rundown of the channel[24]), lack of enough data to formulate a reliable model (eg, dependence on pH_i[25,36,37] and on other nucleotides[25,38] and effects of $[Mg^{2+}]$ on the fraction of open channels[39]), or lack of agreement between different authors (eg, dependence on lactate[25,40]). It is to be noted that the effects of some of these factors, particularly the effects of acidosis, could be of considerable importance in hypoxic/ischemic situations.

To our knowledge, only a few authors have incorporated a model of $I_{K\text{-}ATP}$ in an AP model and used it to study the effect of $I_{K\text{-}ATP}$ activation in cardiac myocytes. Nichols and Lederer[12] incorporated a formulation of $I_{K\text{-}ATP}$ into the model of rat ventricular AP described by Noble.[41] This formulation included only the dependence on $[ATP]_i$, although the dependence on $[ADP]_i$ was implicitly considered. More recently, the incorporation of a model of $I_{K\text{-}ATP}$ that considered dependencies on both $[ATP]_i$ and $[K^+]_o$ to

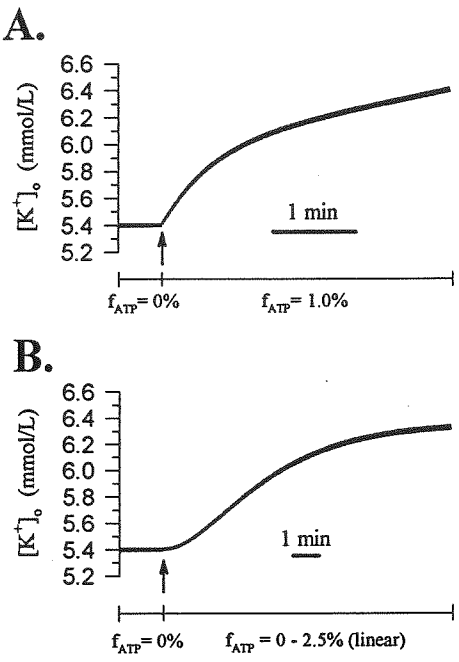

FIG 8. Simulated time course of $[K^+]_o$ after opening of K_{ATP} channels. Values of f_{ATP} during time are represented below each plot. A, Time course of $[K^+]_o$ after an abrupt opening of K_{ATP} channels (f_{ATP}=1.0%). B, Time course of $[K^+]_o$ after a linear increase of f_{ATP} from 0% to 2.5%. Note the different time scales in both panels.

an AP model has been reported.[42] In a different context, Cook et al[10] used a simple computer model to explain the spare-channel hypothesis for beta pancreatic cells. Our description of $I_{K\text{-}ATP}$ is more comprehensive than these previous attempts, because it considers dependencies on intracellular ionic concentrations and intracellular ADP as well as on $[K^+]_o$ and $[ATP]_i$.

The model used in the present study has several limitations. In its present form, it cannot be used to simulate true ischemia, for it lacks a description of other important ischemia-related phenomena apart from $I_{K\text{-}ATP}$ activation. Among them, the most important one might be the influence of acidosis on ionic currents. Also, intracellular ATP decline, free Mg^{2+} rise, and catecholamine release are known to affect other ionic currents, and this should also be considered in a more complete model. Specifically, a more detailed model of the Na^+-K^+ pump would be desirable to determine net K^+ efflux during metabolic inhibition with more accuracy. In its present version, the pump current dependencies on both $[Na^+]_i$ and $[K^+]_o$ are considered,[21] but the model lacks a description of its dependence on ATP and other metabolically related parameters. The influence of $[Mg^{2+}]_i$ on APD through inward Ca^{2+} channels[43] should also be considered. Finally, other pathophysiologically activated currents (such as the Na^+-activated K^+ current and the free fatty acid–activated K^+ current) also deserve some attention.

Effect of $I_{K\text{-}ATP}$ on APD

The theoretical results obtained with our model are in excellent agreement with the spare-channel hypothesis that was proposed by Cook et al[10] for pancreatic cells and was later extended to cardiac cells, according to which only a very small fraction of the total population of K_{ATP} channels in a myocyte needs to be activated to account for the major electrophysiological changes observed in metabolic impairment. Indeed, according to our model, activation of $<1\%$ of the total number of K_{ATP} channels accounts for a 50% reduction in APD in all situations simulated. The value of $\approx$0.6% obtained for normal ionic concentrations correlates well with the values obtained experimentally using indirect methods, namely, 1%,[11] 0.7%,[13] and 0.41%.[14]

The degree of K_{ATP} channel activation needed to account for a 50% reduction in APD might be easily achieved in early hypoxic and ischemic situations. For example, Weiss et al[14] reported nucleotide levels of $[ATP]_i$=4.3 mmol/L and $[ADP]_i$=95 μmol/L after 10 minutes of substrate-free hypoxia. This would correspond, according to Fig 1B, to f_{ATP}=0.68%. In the same experimental study, 10 minutes of ischemia reduced intracellular ATP to 4.6 mmol/L and increased free cytosolic ADP to 63 to 99 μmol/L, which would yield a value between 0.57% and 0.63% for f_{ATP}. Thus, it is seen that even if intracellular ATP levels fall only modestly during early hypoxia/ischemia, activation of K_{ATP} channels may account for drastic reductions in APD. It is clear that the rise in free cytosolic ADP levels is a key factor to quantitatively explain the APD reduction. Indeed, if $[ADP]_i$ was held constant, f_{ATP} would reach a hypoxic/ischemic value of only $\approx$0.2%, which is far less than the 0.6% needed to reduce APD to half its control value.

Our results also indicate that the fraction of open K_{ATP} channels that exist during normal perfusion causes some degree of "baseline" shortening in the AP, which would theoretically be reversed by applying a perfect K_{ATP} channel blocker. Indeed, using the normoxic values of intracellular ATP and ADP (6.8 mmol/L and 15 μmol/L, respectively) reported by Weiss et al,[14] the normal value of f_{ATP} would be 0.11%. According to Fig 2B, this would cause a reduction in APD to $\approx$88% to 91% of the value it would have in the complete absence of $I_{K\text{-}ATP}$. This result is in agreement with one experimental report[44] but contradicts others regarding the inefficiency of sulfonylureas to prolong APD in normally perfused myocytes.[17,34] If we consider a new reference value for APD that corresponds to f_{ATP}=0.11%, then the fraction of open channels needed to be activated to reduce APD to 50% of its normal value would now be $\approx$0.7% instead of 0.6%.

Regarding the influence of intracellular cations on the AP shortening caused by $I_{K\text{-}ATP}$, the results of our model show that pathophysiological levels of Mg^{2+} exert a strong influence on APD, whereas the direct (K_{ATP}-related) effect of Na^+ is much less noticeable. Intracellular free Mg^{2+} is known to rise in early ischemia,[33] and this would reduce the K_{ATP}-mediated effects of ATP depletion on APD (Fig 4). However, high levels of intracellular Mg^{2+} are known to significantly shorten APD by reducing Ca^{2+} inward currents.[43] Thus, elevated free $[Mg^{2+}]_i$ would have at least two opposite effects on APD, with K_{ATP}-dependent effects partially counteracting Ca^{2+} current–dependent APD shortening.

As for the reduction of APD caused by increased Na^+ levels (Fig 5B), it is mainly due to an enhanced activity of the Na^+-K^+ pump as a response to high $[Na^+]_i$, being practically independent of K_{ATP} channel activity. This effect is not likely to be physiologically significant: the extent to which $[Na^+]_i$ increases during early ischemia is not unanimously established,[20] and whether the activity of the electrogenic Na^+-K^+ pump is enhanced or depressed during

the first phase of ischemia and hypoxia is still not completely determined.[20]

Effects of $I_{K\text{-}ATP}$ Activation and High $[K^+]_o$ in Ischemic AP Shortening

The question of the contribution of high extracellular K^+ and of K_{ATP} channel activation to AP shortening is still being debated. Although it is generally accepted that $I_{K\text{-}ATP}$ activation is the key factor in ischemic APD reduction,[11-15] experimental evidence exists that questions this hypothesis.[4,7-9] According to a recent report by Yan et al,[4] ischemic AP shortening would be due to high $[K^+]_o$, and the role of $I_{K\text{-}ATP}$ in this matter would be irrelevant because K_{ATP} channels would not become activated at all. The reduction of APD following extracellular K^+ accumulation is due to the $[K^+]_o$-dependent change of the current-voltage relation. Indeed, elevated levels of $[K^+]_o$ produce an increase in both the delayed rectifier current (I_K) and the inward rectifier current (I_{K1}) because their conductance increases with $[K^+]_o$ according to a square-root law[21] and rectification is partially relieved. This elevation in outward current accelerates repolarization, thus leading to a shortening in APD.

The results of Yan et al,[4] however, show that hypoxia with high $[K^+]_o$ produces an additional shortening of the AP that is not due to high $[K^+]_o$ only (see Fig 7 of Reference 4). This result has also been obtained in another experimental study.[45] According to our theoretical results, a very low degree of K_{ATP} channel activation may easily account for this additional APD reduction. Indeed, both high $[K^+]_o$ and $I_{K\text{-}ATP}$ activation cooperate to shorten AP (see Fig 6). In the complete absence of $I_{K\text{-}ATP}$ activation, the Luo-Rudy model[21] predicts a reduction of relative APD from 100% to 71% when $[K^+]_o$ rises from 4.0 to 10.3 mmol/L, which is in very good agreement with the value reported by Yan. Given this $[K^+]_o$, <0.2% of the total population of K_{ATP} channels would need to open to account for the additional APD reduction (58%) observed by Yan. This degree of activation would in turn be achieved even with very modest variations in intracellular nucleotide concentrations.

In another study, Kodama et al[45] observed that the reduction in APD caused by substrate-free hypoxia with a high $[K^+]_o$ was similar to that obtained under normal $[K^+]_o$. If the data of their Table 1 regarding APD at 80% repolarization are normalized in the same manner as in Fig 6C, it can be deduced that the normalized APD values for different $[K^+]_o$ for 10 and 15 minutes of hypoxia are practically independent of the value of $[K^+]_o$. Our results illustrated in Fig 6C are in agreement with this observation. Moreover, their results regarding APD reduction in different degrees of hyperkalemia under normoxic and hypoxic conditions (see their Table 1) nicely agree with the results of our model (partially depicted in Fig 6B), suggesting that the hypoxia-related AP shortening is mainly due to the activation of $I_{K\text{-}ATP}$.

Ischemic K^+ Loss and Extracellular K^+ Accumulation

Our results support the idea that K_{ATP} channel activation does not fully account for the observed cellular K^+ loss during hypoxia/ischemia. The model predicts the existence of a net increment in J_{efflux} in hypoxia/ischemia, but its magnitude is significantly lower than that observed experimentally (Fig 7C and 7D). Qualitatively, though, our model predicts the well-known plateau of $[K^+]_o$ during the early phase of ischemia (see Fig 8B). According to our results, this plateau is reached because of the biphasic behavior of ΔJ_{efflux} (Fig 7A and 7B). Initially, activation of K_{ATP} channel causes an increase in ΔJ_{efflux}, but after a certain value of f_{ATP} is reached, this trend changes and ΔJ_{efflux} declines until it reaches zero value. This would cause a stabilization of $[K^+]_o$, as shown in Fig 8B.

However, our simulations show that the fraction of the total K^+ loss attributable to $I_{K\text{-}ATP}$ would be in the range of 1/5 (Fig 7D), and so other mechanisms must account for the bulk of the observed K^+ loss. Other possible mechanisms of K^+ loss include changes in other currents during metabolic impairment, activation of other K^+ channels during ischemia (such as the Na^+-activated K^+ channel), cotransport of lactate or Cl^- anions, or extracellular space shrinkage, among others (see Reference 20 for a review).

The results obtained with the model are in partial disagreement with one experimental result, which suggests that a degree of K_{ATP} channel activation of <0.5% would account for the observed hypoxic/ischemic K^+ loss.[14] However, the model predictions dealing with the participation of $I_{K\text{-}ATP}$ in ischemic K^+ loss agree nicely with other reported experimental values regarding the partial prevention of K^+ loss in ischemia by glibenclamide. For example, the data from Hicks and Cobbe[46] indicate that the glibenclamide-prevented extracellular K^+ accumulation during 30 minutes of global ischemia in rabbit septum reached 4.1 mmol/L, a value equivalent to an average ΔJ_{efflux} of 0.071 $\mu mol \cdot g^{-1} \cdot min^{-1}$ (using the value V_{ECW}=0.52 L/kg wet wt reported by Weiss et al[30]), which is in the range of values predicted by our model (see Fig 7D). In a study by Yan et al,[4] glibenclamide reduced K^+ efflux from 4.51 to 3.47 μmol/g wet wt in a 15-minute period of hypoxia with high $[K^+]_o$. This yields a value of 0.069 $\mu mol \cdot g^{-1} \cdot min^{-1}$ for the average ΔJ_{efflux} due to the glibenclamide-blocked currents (mainly $I_{K\text{-}ATP}$), which is again in accordance with the predictions of the model.

Sensitivity of the Results to Model Parameters

One important issue regarding computer models that must always be taken into consideration is the sensitivity of the results to the values of the model parameters. In the model of $I_{K\text{-}ATP}$ presented here, parameters are, in general, well matched to experimental measurements. The parameter that shows the greatest dispersion when measured experimentally is the [ATP] of half-maximum inhibition of the channel (K_m in Equation 4).[14,26] However, its value does not influence our conclusions because the results are presented in terms of f_{ATP}.

Another parameter that could have influence in the quantitative results, because it multiplies f_{ATP} in Equation 1, is the K_{ATP} channel density (σ). The value chosen (3.8 channels/μm^2, derived from Reference 14) lies in the middle of the range of reported values for guinea pig ventricular myocytes. Figures as low as 0.55 channel/μm^2 have been reported,[47] and if this value were to be adopted, all the results regarding the value of f_{ATP} should be multiplied by a factor of 7, so the results of the present study would be compromised. However, all subsequent estimates of the parameter σ yielded considerably higher values. If the estimate of Nichols et al[13] ($\approx$5 channels/μm^2, which is the highest value reported for guinea pig cardiac cells) is taken into consideration, the values of f_{ATP} given in the present study would actually be 1.3 times smaller (eg, f_{ATP} needed for a 50% reduction in APD would now be 0.45%). Thus, all qualitative results would still withstand this examination.

As for the values obtained for K^+ efflux, Equation 6 shows that the results are critically dependent on the chosen V_{ECW}, which has a rather uncertain value. The value chosen for V_{ECW} (0.52 L/kg wet wt) is typical for rabbit septa.[30] Values as low as 0.2 have been reported for other animal species. If this value of 0.2 L/kg wet wt was adopted, the results obtained regarding K^+ efflux rates would have been 66% higher. Even in this extreme case, the simulated values of ΔJ_{efflux} would still be on the order of 3 to 4 times lower than the reported experimental results.

Appendix 1: Formulation of $I_{K\text{-}ATP}$

General Equation

The general equation that describes the total current density through the K_{ATP} channels is the following:

$$I_{K\text{-}ATP}=\sigma g_0 p_o f_{ATP}(V_m-E_{K\text{-}ATP}) \quad (8)$$

where σ is the channel density, g_0 is the unitary conductance, p_o is the maximum channel open probability (in the absence of ATP), f_{ATP} is the fraction of open K_{ATP} channels, V_m is membrane potential, and $E_{K\text{-}ATP}$ is the reversal potential.

The value chosen for the channel density was $\sigma=3.8$ channels/μm^2, and p_o was fixed at a value of 0.91.

Unitary Conductance

The expression for the conductance of a single fully open channel is as follows:

$$g_0=\gamma_0 f_M f_N f_T \quad (9)$$

The term γ_0 is the unitary conductance in the absence of intracellular Na^+ and Mg^{2+} and depends on $[K^+]_o$:

$$\gamma_0=35.375\left(\frac{[K^+]_o}{5.4}\right)^{0.24} \quad (10)$$

where γ_0 is obtained in pS ($[K^+]_o$ in mmol/L).

The term f_M in Equation 9 accounts for inward rectification caused by intracellular Mg^{2+} ions and is formulated by means of a Hill equation:

$$f_M=\frac{1}{1+\frac{[Mg^{2+}]_i}{K_{h,Mg}}} \quad (11)$$

where the half-maximum saturation constant ($K_{h,Mg}$) depends on membrane potential and on $[K^+]_o$:

$$K_{h,Mg}=K_{h,Mg}([K^+]_o)\exp\left(-\frac{2\delta_{Mg}F}{RT}V_m\right) \quad (12)$$

with the value of the electrical distance (δ_{Mg}) being 0.32. F is the Faraday constant, R is the gas constant, and T is the absolute temperature. The factor $K^0_{h,Mg}$ is given by the following:

$$K_{h,Mg}([K^+]_o)=0.65/\sqrt{[K^+]_o+5} \quad (13)$$

(both $K^0_{h,Mg}$ and $[K^+]_o$ in mmol/L).

The term f_N in Equation 9 accounts for inward rectification caused by intracellular Na^+ ions and is again formulated by means of a Hill equation:

$$f_N=\frac{1}{1+\left(\frac{[Na^+]_i}{K_{h,Na}}\right)^2} \quad (14)$$

where the value of the half-maximum saturation constant ($K_{h,Na}$) depends on membrane voltage:

$$K_{h,Na}=K_{h,Na}\exp\left(-\frac{\delta_{Na}F}{RT}V_m\right) \quad (15)$$

The value adopted for electrical distance (δ_{Na}) is 0.35, whereas $K^0_{h,Na}$ is 25.9 mmol/L.

Finally, the temperature (T) effect was introduced in Equation 9 according to the following expression:

$$f_T(T)=Q_{10}^{(T-T_0)/10} \quad (16)$$

where Q_{10}, T, and T_0 indicate temperature coefficient, absolute temperature, and reference temperature, respectively, with $Q_{10}=1.3$ and $T_0=36°C$.

Fraction of Activated K_{ATP} Channels

In the model, the term f_{ATP} in Equation 8 depends on concentrations of intracellular ATP and of free cytosolic ADP, according to the following expression:

$$f_{ATP}=\frac{1}{1+([ATP]_i/K_m)^H} \quad (17)$$

where both the maximum-inhibition constant (K_m) and the Hill coefficient (H) depend on $[ADP]_i$. The equations that express these dependencies are as follows:

$$K_m=35.8+17.9[ADP]_i^{0.256} \quad (18)$$

(with K_m in μmol/L and $[ADP]_i$ in μmol/L) and

$$H=1.3+0.74\exp(-0.09[ADP]_i) \quad (19)$$

($[ADP]_i$ in μmol/L).

Reversal Potential

The reversal potential of the K_{ATP} channel ($E_{K\text{-}ATP}$) is equal to the equilibrium potential for K^+ and is thus given by the Nernst equation:

$$E_{K\text{-}ATP}=\frac{RT}{F}\log\left(\frac{[K^+]_o}{[K^+]_i}\right) \quad (20)$$

Appendix 2: Calculation of K^+ Efflux

Calculation of the Average K^+ Outward Current Density

The total instantaneous K^+ current density ($I_{K,T}$) through the membrane is the sum of all the sarcolemmal currents carried by K^+ ions. In the LR-II model, this is expressed as follows:

$$I_{K,T}=I_{Ca,K}+I_K+I_{K1}+I_{Kp}-2I_{NaK}+I_{ns,K}+I_{K\text{-}ATP} \quad (21)$$

Subtracting the inward current carried by the Na^+-K^+ pump from the total K^+ current, we obtain the total outward K^+ current ($I_{K,O}$):

$$I_{K,O}=I_{Ca,K}+I_K+I_{K1}+I_{Kp}+I_{ns,K}+I_{K\text{-}ATP} \quad (22)$$

The average outward current density (I_{out}) was then calculated as the integral mean value of $I_{K,O}$:

$$I_{out}=\frac{1}{BCL}\int_0^{BCL} I_{K,O}dt \quad (23)$$

Derivation of Equation 6

The K^+ efflux rate (J_{efflux}) can be defined as the number of moles of K^+ leaving the cell (n_{out}) per unit time (Δt) and unit tissue weight (Δm):

$$J_{efflux}=\frac{n_{out}}{\Delta t \Delta m} \quad (24)$$

The number of moles of n_{out} can be related to the electric charge carried by K^+ ions leaving the cell (Q_{out}) by means of the

Faraday constant ($n_{out}=Q_{out}/F$). Along with this, Q_{out} is related to the average K^+ outward current density (I_{out}) as

$$Q_{out}=I_{out}A_m\Delta t \tag{25}$$

where A_m is the total membrane area of all the myocytes contained in the tissue of unit mass Δm.

Rearranging the equations, we obtain the following:

$$J_{efflux}=\frac{A_m}{F\Delta m}I_{out} \tag{26}$$

Now the total membrane area (A_m) can be related to the total cell volume (V_{cel}) by means of the surface-to-volume ratio of the myocyte (S_v): $A_m=V_{cel}\cdot S_v$. Moreover, V_{cel} can be expressed as the difference between the total tissue volume (V_t) and the volume occupied by the extracellular water (V_e). Thus, we obtain the following:

$$J_{efflux}=\frac{S_v(V_t-V_e)}{F\Delta m}I_{out}=\frac{S_v}{F}\left[\frac{1}{(\Delta m/V_t)}-\frac{V_e}{\Delta m}\right]I_{out} \tag{27}$$

The term $\Delta m/V_t$ in the previous equation is the tissue density (ρ), and the term $V_e/\Delta m$ is the extracellular water content per unit weight (V_{ECW}). This yields the following:

$$J_{efflux}=\frac{S_v}{F}\left[\frac{1}{\rho}-V_{ECW}\right]I_{out} \tag{28}$$

Finally, if we want to express J_{efflux} in $\mu mol\cdot g^{-1}\cdot min^{-1}$ while having S_v in $\mu m^2/\mu m^3$, F in coulomb/mol, ρ in g/cm^3, V_{ECW} in mL/g, and I_{out} in $\mu A/cm^2$, then a unit conversion factor of 600 000 is needed in Equation 25. The resultant equation is identical to Equation 6 in the text.

Acknowledgments

This study was supported in part by the Conselleria de Educación y Ciencia de la Generalitat Valenciana (Programa de Formación, Perfeccionamiento y Movilidad de Profesores e Investigadores 94/4158). The authors would like to thank Dr Vicente Lopez Merino for helpful discussions.

References

1. Trautwein W, Gottstein U, Dudel J. Der aktionsstrom der myokardfaser im sauerstoffmangel. *Pflugers Arch.* 1954;260:40-60.
2. Wit AL, Janse MJ. *The Ventricular Arrhythmias of Ischemia and Infarction: Electrophysiological Mechanisms.* New York, NY: Futura Publishing Co Inc; 1993:86-87/207-208.
3. Morena H, Janse MJ, Fiolet JWT, Krieger WJG, Crijns H, Durrer D. Comparison of the effects of regional ischemia, hypoxia, hyperkalemia and acidosis on intracellular and extracellular potentials and metabolism in the isolated porcine heart. *Circ Res.* 1980;46:634-646.
4. Yan G-X, Yamada KA, Kléber AG, McHowat J, Corr PB. Dissociation between cellular K^+ loss, reduction in repolarization time, and tissue ATP levels during myocardial hypoxia and ischemia. *Circ Res.* 1993;72:560-570.
5. Vleugels A, Vereecke J, Carmeliet E. Ionic currents during hypoxia in voltage-clamped cat ventricular muscle. *Circ Res.* 1980;47:501-508.
6. Noma A. ATP-regulated K channels in cardiac muscle. *Nature.* 1983;305:147-148.
7. Elliot AC, Smith GL, Allen DG. Simultaneous measurements of action potential duration and intracellular ATP in isolated ferret hearts exposed to cyanide. *Circ Res.* 1989;64:583-591.
8. De Lorenzi F, Cai S, Schanne OF, Ruiz-Petrich E. Partial contribution of the ATP-sensitive K^+ current to the effects of mild metabolic depression in rabbit myocardium. *Mol Cell Biochem.* 1994;132:133-143.
9. Nakaya H, Takeda Y, Tohse N, Kanno M. Effects of ATP-sensitive K^+ channel blockers on the action potential shortening in hypoxic and ischaemic myocardium. *Br J Pharmacol.* 1991;103:1019-1026.
10. Cook DL, Satin LS, Ashford LJ, Hales N. ATP-sensitive K^+ channels in pancreatic J-cells: spare-channel hypothesis. *Diabetes.* 1988;37:495-498.
11. Faivre JF, Findlay I. Action potential duration and activation of ATP-sensitive K^+ current in isolated guinea-pig ventricular myocytes. *Biochim Biophys Acta.* 1990;1029:167-172.
12. Nichols CG, Lederer WJ. The regulation of ATP-sensitive K^+ channel activity in intact and permeabilized rat ventricular myocytes. *J Physiol (Lond).* 1990;423:91-110.
13. Nichols CG, Ripoll C, Lederer WJ. ATP-sensitive potassium channel modulation of the guinea pig ventricular action potential and contraction. *Circ Res.* 1991;68:280-287.
14. Weiss JN, Venkatesh N, Lamp ST. ATP-sensitive K^+ channels and cellular K^+ loss in hypoxic and ischaemic mammalian ventricle. *J Physiol (Lond).* 1992;447:649-673.
15. Gasser RNA, Vaughan-Jones RD. Mechanism of potassium efflux and action potential shortening during ischaemia in isolated mammalian cardiac muscle. *J Physiol (Lond).* 1990;431:713-741.
16. Kantor PF, Coetzee WA, Carmeliet EE, Dennis SC, Opie LH. Reduction of ischemic K^+ loss and arrhythmias in rat hearts: effect of glibenclamide, a sulfonylurea. *Circ Res.* 1990;66:478-485.
17. Wilde AAM, Escande D, Schumacher CA, Thuringer D, Mestre M, Fiolet JWT, Janse MJ. Potassium accumulation in the globally ischemic mammalian heart: a role for the ATP-sensitive potassium channel. *Circ Res.* 1990;67:835-843.
18. Vanheel G, De Hemptinne A. Influence of K_{ATP} channel modulation on net potassium efflux from ischaemic mammalian cardiac tissue. *Cardiovasc Res.* 1992;26:1030-1039.
19. Wilde AAM, Schumacher C, Fiolet J, Opthof T, Janse MJ. Mere opening of K_{ATP} channels does not contribute to accumulation of K^+ in the globally ischemic rabbit heart. *J Mol Cell Cardiol.* 1992;24(suppl I):S276. Abstract.
20. Wilde AAM, Aksnes G. Myocardial potassium loss and cell depolarisation in ischaemia and hypoxia. *Cardiovasc Res.* 1995;29:1-15.
21. Luo C-H, Rudy Y. A dynamic model of the cardiac ventricular action potential, I: simulations of ionic currents and concentration changes. *Circ Res.* 1994;74:1071-1096.
22. Kakei M, Noma A, Shibasaki T. Properties of adenosine-triphosphate-regulated potassium channels in guinea-pig ventricular cells. *J Physiol (Lond).* 1985;363:441-462.
23. Horie M, Irisawa H, Noma A. Voltage-dependent magnesium block of adenosine-triphosphate-sensitive potassium channel in guinea-pig ventricular cells. *J Physiol (Lond).* 1987;387:251-272.
24. Trube G, Hescheler J. Inward-rectifying channels in isolated patches of heart cell membrane: ATP-dependence and comparison with cell-attached patches. *Pflugers Arch.* 1984;401:178-184.
25. Lederer WJ, Nichols CG. Nucleotide modulation of the activity of rat heart ATP-sensitive K^+ channels in isolated membrane patches. *J Physiol (Lond).* 1989;419:193-211.
26. Findlay I, Faivre JF. ATP-sensitive K channels in heart muscle: spare channels. *FEBS Lett.* 1991;279:95-97.
27. Terzic A, Tung RT, Kurachi Y. Nucleotide regulation of ATP sensitive potassium channels. *Cardiovasc Res.* 1994;28:746-753.
28. Findlay I. Effects of ADP upon the ATP-sensitive K^+ channel in rat ventricular myocytes. *J Membr Biol.* 1988;101:83-92.
29. Mogul DJ, Singer DH, Ten Eick RE. Dependence of Na-K pump current on internal Na in mammalian cardiac myocytes. *Am J Physiol.* 1990;259:H488-H496.
30. Weiss JN, Lamp ST, Shine KI. Cellular K^+ loss and anion efflux during myocardial ischemia and metabolic inhibition. *Am J Physiol.* 1989;256:H1165-H1175.
31. Gear CW. The automatic integration of stiff ordinary differential equations. In: Morrel AJH, ed. *Information Processing.* Amsterdam, Netherlands: North Holland; 1969.
32. Lederer WJ, Nichols CG, Smith GL. The mechanism of early contractive failure of isolated rat ventricular myocytes subjected to complete metabolic inhibition. *J Physiol (Lond).* 1989;413:329-349.
33. Borchgrevink PC, Bergan AS, Bakøy OE, Jynge P. Magnesium and reperfusion of ischemic rat heart as assessed by ^{31}P-NMR. *Am J Physiol.* 1989;256:H195-H204.
34. Venkatesh N, Lamp ST, Weiss JN. Sulfonylureas, ATP-sensitive K^+ channels, and cellular K^+ loss during hypoxia, ischemia, and metabolic inhibition in mammalian ventricle. *Circ Res.* 1991;69:623-637.
35. Kléber AG. Extracellular potassium accumulation in acute myocardial ischemia. *J Mol Cell Cardiol.* 1984;16:389-394.
36. Fan Z, Makielski JC. Intracellular H^+ and Ca^+ modulation of trypsin-modified ATP-sensitive K^+ channels in rabbit ventricular myocytes. *Circ Res.* 1993;72:715-722.
37. Fan Z, Furukawa T, Sawanobori T, Makielski JC, Hiraoka M. Cytoplasmic acidosis induces multiple conductance states in ATP-sensitive potassium channels of cardiac myocytes. *J Membr Biol.* 1993;136:169-179.
38. Terzic A, Findlay I, Hosoya Y, Kurachi Y. Dualistic behaviour of ATP-sensitive K^+ channels toward intracellular nucleoside diphosphates. *Neuron.* 1994;12:1049-1058.

39. Findlay I. ATP-sensitive K^+ channels in rat ventricular myocytes are blocked and inactivated by internal divalent cations. *Pflugers Arch.* 1987;410:313-320.
40. Keung EC, Li Q. Lactate activates ATP-sensitive potassium channels in guinea pig ventricular myocytes. *J Clin Invest.* 1991;88:1772-1777.
41. Noble D. *Oxsoft Heart Program Manual (Version 2.1).* Oxford, UK: OXSOFT Ltd; 1988.
42. Shaw R, Rudy Y. Electrophysiological changes of ventricular tissue under ischemic conditions: a simulation study. *Comp Cardiol.* 1994; 16:641-644.
43. Agus ZS, Kelepouris E, Dukes I, Morad M. Cytosolic magnesium modulates calcium channel activity in mammalian ventricular cells. *Am J Physiol.* 1989;256:C452-C455.
44. Faivre JF, Findlay I. Effects of tolbutamide, glibenclamide and diazoxide upon action potentials recorded from rat ventricular muscle. *Biochim Biophys Acta.* 1989;984:1-5.
45. Kodama I, Wilde AAM, Janse MJ, Durrer D, Yamada K. Combined effects of hypoxia, hyperkalemia and acidosis on membrane action potential and excitability of guinea-pig ventricular muscle. *J Mol Cell Cardiol.* 1984;16:247-259.
46. Hicks MN, Cobbe SM. Effect of glibenclamide on extracellular potassium accumulation and the electrophysiological changes during myocardial ischaemia in the arterially perfused interventricular septum of rabbit. *Cardiovasc Res.* 1991;25:407-413.
47. Noma A, Shibasaki T. Membrane current through adenosine-triphosphate-regulated potassium channels in guinea-pig ventricular cells. *J Physiol (Lond).* 1985;363:463-480.